

T.YA. GORBACH, P.S. SMERTENKO, E.F. VENGER

V.E. Lashkaryov Institute of Semiconductor Physics, Nat. Acad. of Sci. of Ukraine  
(45, Prosp. Nauky, Kyiv 03680, Ukraine; e-mail: smertenko@isp.kiev.ua)

## INVESTIGATION OF PHOTOVOLTAIC AND OPTICAL PROPERTIES OF SELF-ORGANIZED ORGANIC-INORGANIC HYBRIDS USING AROMATIC DRUGS AND PATTERNED SILICON

PACS 33.80.-b, 78.20.-e,  
89.30.Cc

The effect of incorporation of the functional groups of aromatic molecules onto the Si surface has been investigated by photovoltaic (PV) and photoluminescence (PL) characteristics, infrared (IR) spectroscopy, scanning electron microscopy (SEM), and optical microscopy (OM). To realize the organic-inorganic hybrids, the thin (10–100 nm) layers of heteroatom aromatic pharmaceutical drugs (APD) such as clonidine hydrochloride (CLON), procainamide hydrochloride (PRO), and cyanocobalamin (CYCAM – B<sub>12</sub> vitamin) were formed by the chemical solution deposition process on the Si patterned surface at room temperature under laboratory ambient conditions. The hybrids have shown: (i) the solar energy conversion with an efficiency up to 6–7% in dependence on the chemical solution media and the surface and interface morphologies; (ii) the highest efficiency of 8.4% in CLON–Si hybrids produced in a mixed solution with a layer 30 nm in thickness and a self-organized net-like surface morphology; (iii) the intense photoluminescence in the waverange of 400–900 nm, luminescence profile, and peak position suggest the vibronic origin of this band; (iv) the presence of characteristic bands associated to the functional groups containing nitrogen (amines NH<sub>x</sub> ( $x = 0, 1, 2$ ), amides OCN, cyanonitrile CN), carbon and/or hydrogen-hydrocarbons (CH<sub>x</sub> ( $x = 1, 2, 3$ )), oxygen (hydroxyl OH, peptide CO), halogens (chloroalkane) and phosphorus (phosphate OPO(OH)<sub>2</sub>). Possible principles of operation of APD–Si hybrids are discussed.

**Keywords:** aromatic drugs, patterned silicon, photovoltaic and photoluminescence characteristics, infrared spectroscopy, scanning electron microscopy, optical microscopy, clonidine hydrochloride, procainamide hydrochloride, cyanocobalamin.

### 1. Introduction

Organic modification, functionalization, and sensitization of silicon have increased enormously during the last few years [1–3]. Such resulting organic-inorganic hybrids have attracted a great interest for physics, chemistry, as well as for innovative research areas in biology and medicine. They are potential objects for photovoltaics, optoelectronics, biosensing, and gene and drug delivery applications due to: (i) unique properties of both the isolated molecule and self-organized molecular assemblies or aggregations; (ii) the combination of a high absorption coefficient of organics and good Si transport properties; (iii) hybrid compatibility with well explored Si planar technology [4–12].

It should be noted that, in the most cases, the etched, oxidized, diffused, implanted, and homo-heteroepitaxial Si surfaces are functionalized or multifunctionalized. Among them, electrochemically etched porous silicon, anisotropically acidic or alkaline etched patterned Si, reconstructed hydride and halide terminated surface of Si have other properties (reflection, transmission, visible luminescence, *etc.*) than flat ones. Such very successful functionalization has been obtained by inorganic processes as a result of the technological, technical, and physical requirements and practical device applications [13–16].

Now, the new opportunities are opening in micro/nanometer-size silicon based devices of the next generation with unprecedented level of functionality based on various reactions of Si with organic materials including organometallic and aromatic systems [1–3].

It was reported [17–22] that the hybrid heterostructures based on phthalocyanines (Au–pMgPc–

© T.YA. GORBACH, P.S. SMERTENKO,  
E.F. VENGER, 2014

$n$ Si, Au- $p$ ZnPc- $n$ Si and Au- $p$ ZnPc- $p$ Si) and porphyrins (TPPS<sub>4</sub> (mesotetra (4-sulfonato phenyl porphyrine) – crystalline Si{100}/Si{111}, Fe-TPPS<sub>4</sub>-Si, and ZnTPP (Zn mesotetraphenyl porphyrine) – Si{111}:H) showed a rectification behavior, photovoltaic (PV) characteristics with conversion efficiencies in the range of 0.74–2.3%, morphological and optical features. Sensitization of  $\alpha$ -Si and  $\mu$ c-Si was shown by photoconductivity measurements [19].

Cases of hybrids with organic materials organized by biomolecules have been presented in [9–12, 23–27]. They are of special and specific interest for biomedical applications. This is one of the arguable topics these days. Among the best examples to illustrate these positions are:

(i) immobilization of a functionalized Si substrate with organometallic NH<sub>2</sub>(CH<sub>2</sub>)<sub>3</sub>Si(OC<sub>2</sub>H<sub>5</sub>)<sub>3</sub> by antibodies (immunoglobulines) [23],

(ii) functionalization of a misoriented dislocation Si with protein and DNA molecules [24],

(iii) realization of the porous Si product known as Bio-Silicon in pharmaceutical and medical researches ranging from controlled drug delivery, clinical diagnostics, tissue engineering, *etc.* [9–12, 25].

The positive effect of deposited vitamin B<sub>1</sub> (thiamine diphosphate hydrochloride) and other drugs on patterned  $n^+p$ Si structures of solar cells has already been described in our work earlier [28]. The  $n^+p$ Si solar cells with Eff  $\leq$  5–7% result in Eff up to 15% in the novel drug-Si hybrid system. The later deposition of B<sub>1</sub> and metamisol sodium on patterned  $n$ Si and the testing of PV parameters have showed that these drugs-Si hybrids have the efficiency of solar energy conversion of about 1.0% under AM 1.5 and 0.3 Sun, respectively [29].

However, the presented picture is based upon a very limited range of hybrid systems, and the good performance of solar cells remains the open question.

In order that the idea of using drugs in both photovoltaics and a variety of healthcare applications be implemented, the further study and investigation should be focused on another drug-Si systems.

It is known that the most important building block of many organic materials are aromatics. They include both the simplest classical six-membered aromatic ring of benzene molecules and five- and six-membered rings containing heteroatoms such as pyrrole, thiazole, pyridine, *etc.* A very large number of pharmaceutical drugs are aromatics too. In this

study, the elegant examples of therapeutic drugs as the complicated aromatic from the cardiovascular group (antiarrhythmic, antihypertensive) and “bio-functional” vitamin B<sub>12</sub> as an analogue of DNA were chosen for advanced structures of organic layers based on Si.

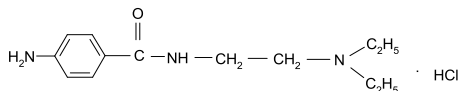
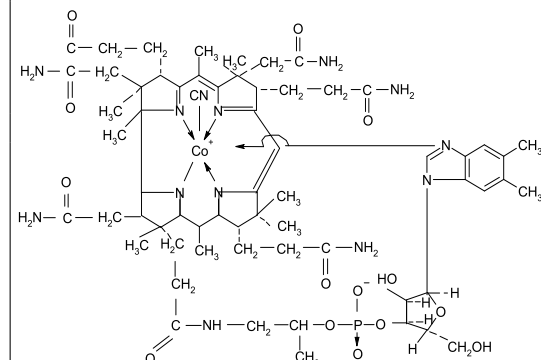
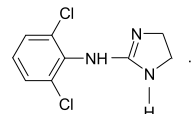
The current investigation is presented in some aspects: (i) a correlation of morphological modification of the functional surface and the interface of drug-Si hybrids processed through chemical bath deposition at room temperature with final hybrid performance for the solar cell application; (ii) understanding of the essence of functionalization and self-assembly model; (iii) investigation of physical-chemical properties and peculiarities of drug-Si hybrids to manipulate and to optimize the photovoltaic parameters in controlled manner of such organic-inorganic systems.

## 2. Experimental

Monocrystalline Czochralski-grown Si wafers with {100} orientation,  $n$ -type conductivity with a dopant concentration of  $10^{15}$ – $10^{16}$  cm<sup>-3</sup>, and an anisotropically etched surface in the form of a tetragonal pyramid were used as a substrate. Such pyramidal patterned (textured) substrates are the standard for photovoltaics [14]. Their technological important feature for the growth of a film is its side facet {111}. The facet {111} is vicinal with surface roughness on the microscopic and nanoscopic levels, where atomically flat, low-Miller index terraces {111} are separated by steps, which, in turn, have the kinks, i.e., the TSK features are revealed. Under the morphological stability condition (stable facet growth), the TSK growth mechanism is realized. In such case, a low-temperature and even room-temperature deposition of a good quality film is possible in spite of the lattice mismatch and a difference in the thermal expansion coefficients of a substrate and a film, for example, GaAs/Si, GaP/Si, CdHgTe/Si, thiamine diphosphate/Si *etc.* [29–31].

Three commercial aromatic pharmaceutical drugs (APD) – procainamide hydrochloride (PRO), clonidine hydrochloride (CLON), cyanocobalamin – vitamin B<sub>12</sub> (CYCAM) used in this study were purchased in pharmacy both in the tablet form and ampoule (Table 1) [32]. In addition, solid B<sub>12</sub> was purchased in a chemist’s shop to obtain the concentrated B<sub>12</sub> solution (to 1.25%) on the contrary pharmaceutical 0.05% solution.

Table 1. List of pharmaceutical drugs, their abbreviations, chemical composition, molecular formula, and additional substances [32]

No.	Title, chemical formula	Molecular formula	Additional substance
1	Procainamide hydrochloride, PRO, (4-amino-N-(2-diethylaminoethyl benzamide)		Tablet: lactose monohydrate (C <sub>12</sub> H <sub>22</sub> O <sub>11</sub> ), starch ([C <sub>6</sub> H <sub>10</sub> O <sub>5</sub> ] <sub>n</sub> ), polyvidone ([C <sub>6</sub> H <sub>9</sub> NO] <sub>n</sub> ), calcium stearate Ampoule: Metabisulphate sodium Na <sub>2</sub> SO <sub>3</sub> , H <sub>2</sub> O
2	Cyanocobalamin, CYCAM, (Coα-[α-(5,6 dimethyl benzimidazole)-Coβ-cobamidcyanide)		H <sub>2</sub> O, NaCl, starch
3	Clonidine hydrochloride, CLON, (N-(2,6-dichlorophenyl)-4,5-dihydro-1H-imidazol-2-amine)		Tablet: lactose monohydrate, starch, magnesium stearate

Although all these drugs are heteroatom aromatics, they differ at least in three main ways. First, both a procainamide molecule and a cyanocobalamin one with amine-amide and imide-amide compositions, respectively, are donor acceptor complexes with charge transfer. In clonidine, the amine-imide composition takes place. This drug may be attributed to organic electron donors.

Second, due to a small molecular length and Cl derivate benzene ring, a clonidine molecule is more conductive than procainamide and cyanocobalamin complexes.

Third, in contrast, procainamide cyanocobalamin is a large pigment-protein complex consisting from structurally and functionally different parts. The basis of cyanocobalamin is a corrin ring which is similar to the porphyrin ring of chlorophyll, heme, and cytochrome. The central metal ion is the rare biochemical element cobalt. It is the center of reactivity and is connected with a dimethylbenzimidazole group and a cyanogroup CN. In addition, this

molecule contains phosphate, methyl, and carboxamide groups. Phosphate group is self-organized, and CN is activated and sensitized.

The periphery of the core-complex and carboxamide- end groups may be attributed to light harvesting (antenna) and transferring the exciting energy into silicon. This extra large aromatic system is the most desirable from the point of view of functionalization in comparison with procainamide and clonidine.

At the same time, among the another factors that determine the choose of PD for hybrid fabrication were: (i) absence of purification and additional doping; (ii) low cost of a material used; (iii) environment-friendly substance; (iv) room-temperature technological process of functionalization of the surface and formation of a hybrid; (v) nontoxic.

Water, organic and mixed solvents consisting of water, and organic solvent in equal volumes were used for the preparation of the solution. Organic and mixed solvents were pentachlorophenol (C<sub>6</sub>HCl<sub>5</sub>O) in methanol (CH<sub>3</sub>OH), carbon tetrachloride (CCl<sub>4</sub>) and

ethanol ( $C_2H_5OH$ ). It should be noted that not all liquid organic media can be regarded as homogeneous chemical media, and their identification as a solution is conditional. In the case of using the tablet forms, the mixture of water and APD contains both additional substances as a lactose monohydrate, starch, polyvidone and ligands as magnesium stearate, calcium stearate, *etc.* Whereas the lactose monohydrate is water-solved, starch and polyvidone are not solved in water. Due to these factors, liquid media of APD obtained from tablets can be referred to the suspensions, most probably. Counting on the basic drug substance the concentrations of PRO and CLON were 0.5% and 0.01%, respectively. Concentration of CYCAM is about 1.25%. Procainamide ampoule has 10-% concentration.

APD-Si hybrids were prepared by the chemical bath deposition at room temperature under ambient laboratory conditions. Deposition was carried out from the above-mentioned chemical media onto the front surface of Si patterned substrates. Rear surface was protected by a chemically stable varnish. Then the substrate was immersed into a glass bath with a chemical solution for the deposition of an organic film. The deposition time was varied in dependence on the chemical medium and its concentration. Ag paint was applied for contact to hybrids.

The morphological images of deposited films and hybrids were characterised by scanning electron microscopy (SEM) and through the optical microscopy (OM). Investigation of functionalization of the Si surface and hybrids was carried out using photovoltaic data (PV), photoluminescence (PL), and IR transmission and reflection spectra.

The PV setup under standard test conditions ( $100\text{ mV/cm}^2$ ,  $25\text{ }^\circ\text{C}$ ) and the global spectrum corresponding to air mass 1.5 were used for the measurement of PV hybrid parameters with  $\pm 2.5\%$  accuracy. The PV monitoring at different irradiances was performed using the same steady state solar stimulator, as in STC and neutral filters, i.e. without a modification of the spectral distribution of the sunlight.

The measurements of PL were performed under excitation by a 337 nm  $N_2$  gas pulse laser (8 ns, 1.5 kW/pulse) detected by a photomultiplier in the 380–900 nm range in the photon count regime.

Infrared spectra were recorded on a Perkin Elmer "Spectrum BX-II" Fourier spectrometer in the 400–8000  $\text{cm}^{-1}$  range.

### 3. Results and Discussion

#### 3.1. Hybrid morphology and the efficiency of solar energy conversion

The first detailed issue of the surface morphologies of an organic layer formed during the room-temperature chemical bath deposition from the water solution of thiamine diphosphate on Si patterned surface was presented in [29]. The hybrids have shown a noticeable morphological deviation from the pyramid form to a net-like one and then to spherules forms branched. Although the desirable high efficiency of solar energy conversion has not achieved, it has become evident that the favorable morphology is the net-like form, and the hybrid quality has to be assessed by the composition of drug molecules and solution media.

Taking, as an example, the hybrids formed by the deposition from clonidine water organic and mixed media onto the Si patterned substrate (Fig. 1, *a*), the influence of the surface morphology of organic layers, its temporal evolution as a key parameter on the hybrid efficiency are illustrated in Fig. 1, *b, c, d*, Figs. 2 and 3. A few representative and uncommon images for layers deposited from CYCAM water and CLON ethanol solutions are shown in Fig. 1, *e, h*, respectively.

As seen in Fig. 1, *b*, at the initial stage of the CLON layer deposition under stable condition of a moving chemical front, the surface morphology of the organic layer and the CLON-Si hybrid copy the patterned morphology of the substrate. In such situation, the TSK growth mechanism is realized due to a vicinal feature of the  $\{111\}$  pyramid-like substrate. With increase of the deposition time, the loss of the growth stability conditions takes place, and the complex branched morphologies are generated (Figs. 1 and 2). First of all, the organic medium demonstrates a filled and partially buried pyramid (Fig. 1, *c, d*, Fig. 2, *a*). Then the circular, square, and rhombic net surface forms are organized (Fig. 2, *b-d, g-i*) as a result of the filament connection of pyramid vertices.

At the next stage, with increasing of the deposition time, i.e. the layer thickness, the Maltese cross and spherulite forms (Fig. 2, *e, f*) are developed as the filament grows in the radial and circular directions. As shown on filament fragments (Fig. 1, *e, f*) of APD deposited, each filament contains the microfibrils, which, in turn, are organized from a chain

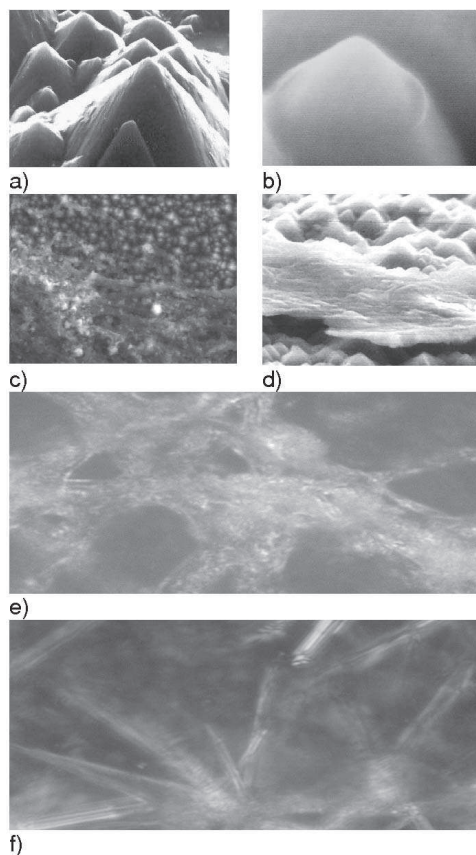


**Fig. 1.** Morphological image of APD-Si surfaces: *a-d* – SEM, *e, f* – OM: *a* – Si patterned substrate, *b, d, f* – surface morphology of CLON-Si hybrids, *c-e* – surface morphology of CYCAM-Si hybrids, *b* – breaking film near the pyramid apex of CLON-Si hybrid, *e-f* – fragments of filaments of CYCAM-Si and CLON-Si hybrids, respectively. 15 mm scale bar presents in: *a, b* – 1  $\mu\text{m}$ , *c, d* – 15  $\mu\text{m}$ , *e, f* – 200 nm

of nanowires and nanodots. Especially, it is seen on hyper branched CYCAM layers (Fig. 1, *e*). With this moment, the layer growth mediated substrate has no preference, and the layer morphology is determined by the self-organized processes.

The interesting morphological phenomenon is observed in hybrid produced in mixed solvent ( $\text{H}_2\text{O} + \text{C}_2\text{H}_5\text{OH}$ ). Morphology is organized by the needle, lamellar, or sometimes quasicylindrically shaped fibers with curving motive (Fig. 1, *f*). Some such forms fork from a common central ball point organized on the pyramid apex. Then after a certain period of time under laboratory conditions, this morphology is self-converted into net-like forms. In other

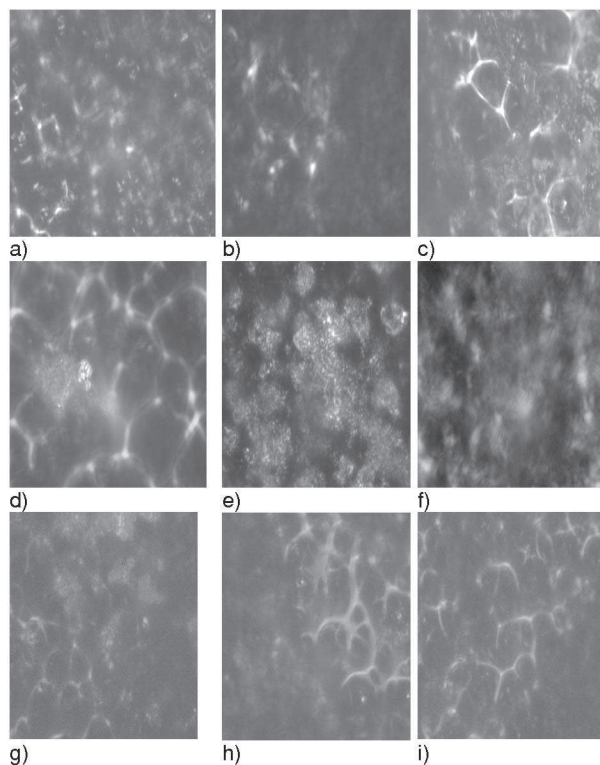


**Fig. 2.** OM photographs of surface morphologies of CLON-Si hybrids deposited from solutions: *a-f* – water, *g* – mixed (water+pentaclorphenole), *h-i* – pentaclorphenol. In the case *h*, CLON was without additional substances. For the water solution, the deposited times are: *a* – 2, *b, c, d* – 3, *e* – 4, *f* – 5 h, respectively. Morphologies of Fig. 2, *g, h* and Fig. 2, *i* are observed after 1 h and 1.5 h depositions, respectively

words, the layer built itself. Thus, the growth nature of these APD layers may be attributed to a molecular self-assembly most probably, although the self-organization and the self-assembly are often used interchangeably, especially in chemistry and biology.

From an overall point of view, these hybrid structures can be considered as synergetic: organizing agent (substrate) and self-assembling molecules (layer).

Comparising the morphological image with PV performance investigations (Fig. 2, 3), it is became obvious that the favor morphology is a net-like form of the surface. But in many cases among a diversity of net-morphologies (Fig. 2, *b-d*), the optimal net-like form is realized as in Fig. 2, *c*. For this morphology, if the CLON deposition takes place from the  $\text{H}_2\text{O}$  solution, then the PV parameters are as follows:  $J_{\text{SC}} = 36.52 \text{ mA/cm}^2$ ,  $V_{\text{OC}} = 0.411 \text{ V}$ ,

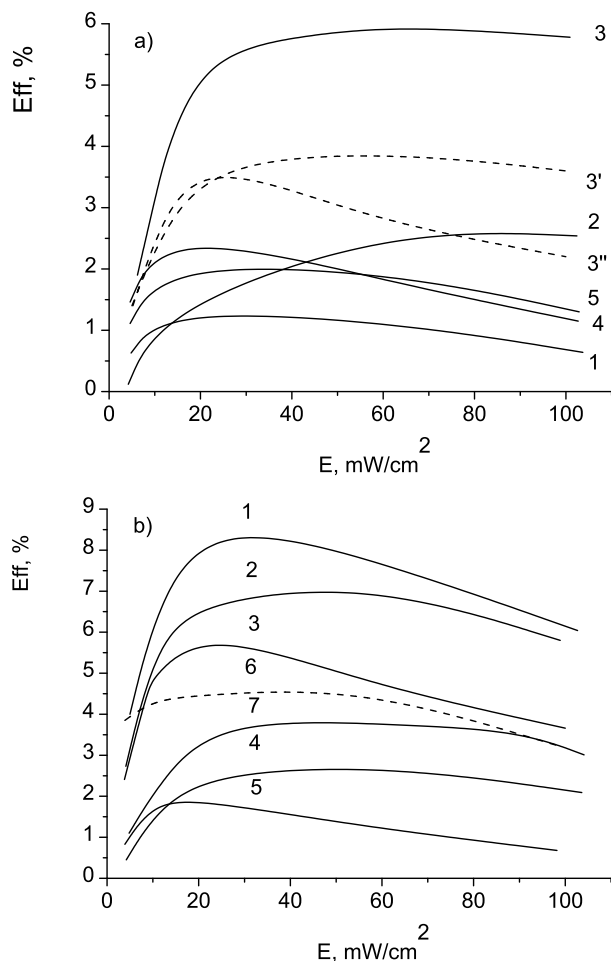


**Fig. 3.** Efficiency versus the power energy irradiance on various deposition times and different morphologies: for CLON-Si hybrids deposited from water (a) and organic and mixed solutions (b) corresponding to the following morphologies: a) curve 1 – Fig. 1, b, curve 2 – Fig. 2, a, curve 3' – Fig. 2, b, curve 3 – Fig. 2, c, curve 3'' – Fig. 2, d, curve 4 – Fig. 2, e, curve 5 – Fig. 2, f; b) for net-like morphologies: curve 1 – H<sub>2</sub>O + C<sub>6</sub>H<sub>5</sub>OH + CH<sub>3</sub>OH; curve 2 – C<sub>6</sub>H<sub>5</sub>OH + CH<sub>3</sub>OH; curve 3 – C<sub>6</sub>H<sub>5</sub>OH + CH<sub>3</sub>OH; and different solution (Fig. 2, g–i) curve 4 – CCl<sub>4</sub>; curve 5 – C<sub>6</sub>H<sub>5</sub>OH + CH<sub>3</sub>OH + H<sub>3</sub>BH<sub>3</sub>; for PRO-Si hybrids (b) curves 6, 7 for CYCAM-Si hybrids, respectively

FF = 0.39, Eff = 5.78% (at AM 1.5), Eff = 5.97% (at 65 mW/cm<sup>2</sup>). Eff versus *E* is shown by curve 3 in Fig 3, a. For other net-morphologies (Fig. 2, b, d), Eff versus *E* is presented by curve 3' and 3'', respectively. PV parameters are: *J*<sub>SC</sub> = 40.00 mA/cm<sup>2</sup>, *V*<sub>OC</sub> = 0.256 V, FF = 0.38, Eff = 3.67% (at AM 1.5),

Eff = 3.98% (at 65 mW/cm<sup>2</sup>) for the net-morphology in Fig. 2, b and *J*<sub>SC</sub> = 36.83 mA/cm<sup>2</sup>, *V*<sub>OC</sub> = 0.203 V, FF = 0.27, Eff = 2.02% (at AM 1.5), Eff = 3.20% (at 20 mW/cm<sup>2</sup>).

From the data of Fig. 3, b, the PV performance and its dependence on the irradiation energy for hybrids with the CLON molecular structure and a net-like morphology have to be functions of solvent media. For example, the CLON deposition from a mixed solvent media containing H<sub>2</sub>O and PCF + CH<sub>3</sub>OH gives *J*<sub>SC</sub> = 40.21 mA/cm<sup>2</sup>, *V*<sub>OC</sub> = 0.438 V, FF = 0.35, Eff = 6.04% under AM 1.5 and Eff<sub>max</sub> = 8.42% at *E* = 25 mW/cm<sup>2</sup>, (Fig. 3, b, curve 1). The morphology is shown in Fig. 2, g. In this solvent medium but without additional substances, the PV parameters of the CLON-Si hybrid with the net morphology (Fig. 2, h) are *J*<sub>SC</sub> = 33.47 mA/cm<sup>2</sup>, *V*<sub>OC</sub> = 0.443 V, FF = 0.39, Eff = 5.79% (at AM 1.5), and Eff = 6.73% (at 60 mW/cm<sup>2</sup>). Eff versus *E* is presented by curve 2 in Fig. 3, b.

For PCF + CH<sub>3</sub>OH solvent, the CLON-Si hybrid has *J*<sub>SC</sub> = 30.00 mA/cm<sup>2</sup>, *V*<sub>OC</sub> = 0.358 V, FF = 0.31, Eff = 3.66% (at AM 1.5) and Eff = 5.71% (at 25 mW/cm<sup>2</sup>) Fig. 3, b, curve 3. The morphology of this structure is shown in Fig. 2, g.

Thus, the combined factors of morphology and solvent mixture give the ability to manipulate the PV efficiency in the APD-*n*-Si hybrid.

### 3.2. Optical properties

#### 3.2.1. Photoluminescence

The PL spectra (Fig. 4) of CLON-Si hybrids with various morphologies have considerable difference both in the peak position and the emission efficiency. According to Fig. 4, a, the hybrids prepared from a water solution possess at least three distinct photoluminescent behaviors as a function of the layer morphology: (i) for a thin layer with the morphology presented in Fig. 1, b, 2, a, the PL spectrum (Fig. 4, a, curve 1) has a single maximum about λ = 450 nm (*E* = 2.75 eV); (ii) for thick layers with branch morphologies (Maltese cross, dendritic-like, Fig. 2, g, f), the peak position situated at λ<sub>1</sub> = 530 nm (*E*<sub>1</sub> = 2.34 eV), i.e. it is displaced in the direction of long wavelengths. In addition, PL intensity (Fig. 4, curve 4) increased essentially; (iii) PL spectra (Fig. 4, a, curve 3) of layers with a net-like morphology (Fig. 2, b, c) more structured. Like this, the

PL spectrum presented by curve 3, contains three luminescence bands with maxima located at 450 nm, 530 nm and 820 nm ( $E = 1.51$  eV).

The spectral dependence of PL for CLON–Si hybrids with a net-like morphology formed in  $\text{CCl}_4$  solution is shown in Fig. 4, *b* (curve 2). Besides curve 1, Fig. 4, *b*, presents the PL spectrum of a CLON layer 50  $\mu$  in thickness separated from the Si substrate. It is possible to observe two maxima in the last spectrum at about 510 nm (2.43 eV) and 600 nm (2.07 eV) in comparison with the single maximum (2.43 eV) of the CLON–Si hybrid. On the contrary, the PL wavelength profile (Fig. 4, *b*, curve 3) of the CLON–Si hybrid formed from the mixed solution ( $\text{H}_2\text{O} + \text{C}_6\text{HCl}_5\text{O}$ ) is changed. The spectrum has three luminescence peaks. The contribution to this PL profile may appear both from PL with peak position at  $\sim 450$  nm (Fig. 4, *a*), as well as from PL of a hybrid produced in the organic solution. An interesting feature of the spectrum is shown in Fig. 4, *b* (curve 4). Meanwhile, this result will not be discussed here.

In the PL spectrum (Fig. 4, *c* (curve 1) of the PRO–Si hybrid, there are at least three luminescent peaks about 440 nm, 530 nm, and 600 nm. The PL spectrum of CYCAM–Si (Fig. 4, *c* (curve 2) hybrid with the net morphology has two maxima: at  $\sim 500$  nm and at  $\sim 800$  nm with two shoulders: a shortwave shoulder at about  $\sim 440$  nm and a longwave one at  $\sim 535$  nm. It may be remarked that the preliminary study of the absorption spectra for the CLON water solution and mixed with pentachlorophenol one has shown that: the absorption edges are 3.8 eV and 3.2 eV, respectively.

Thus, these investigations as well as the PV one, revealed that the Si patterned surface modified with APD has emission properties in 400–800 nm range with some different PL wavelength profile. APD–Si hybrids with min PL intensity have max PV efficiency for the identical net-morphology.

### 3.3. FTIR spectra

It seems attractive to assume that the phenomena similar to the PV and PL properties of APD–Si hybrids investigated and reported in the previous sections are originated from a barrier structure formed by a deposited organic aromatic molecular layer and patterned Si.

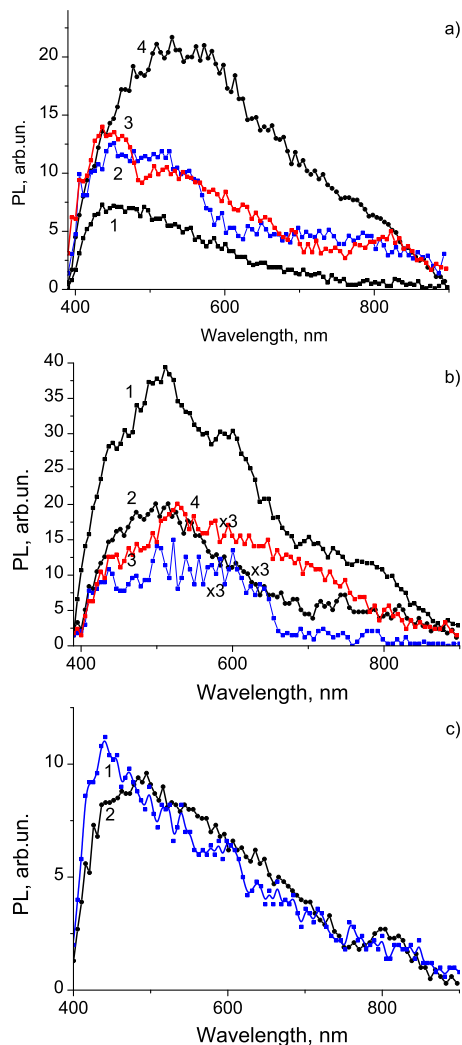


**Fig. 4.** PL spectra of CLON–Si hybrids deposited from water (*a*) and organic and mixed (*b*) solutions in dependence on the time deposition and the surface morphology: *a*) for pyramid-like (curve 1), partially buried pyramids (curve 2), net form (curve 3), spherulite-like (curve 4); *b*) for net-like morphologies, curves 2–4 represent CLON–Si hybrids deposited from  $\text{CCl}_4$ ,  $\text{H}_2\text{O} + \text{C}_6\text{H}_5\text{OH} + \text{CH}_3\text{OH}$ , respectively. On curve 1, PL of a free film deposited from the  $\text{CCl}_4$  solution is shown; *c*) the PL spectra of PRO–Si (curve 1) and CYCAM–Si (curve 2) hybrids

In this section, the vibration modes in IR spectra are investigated to obtain a further information about the functional groups of atoms within APD molecules deposited on Si.

Figure 5, *a* presents the FTIR spectra of a 50  $\mu\text{m}$  layer produced from the CLON/ $\text{CCl}_4$  solution and

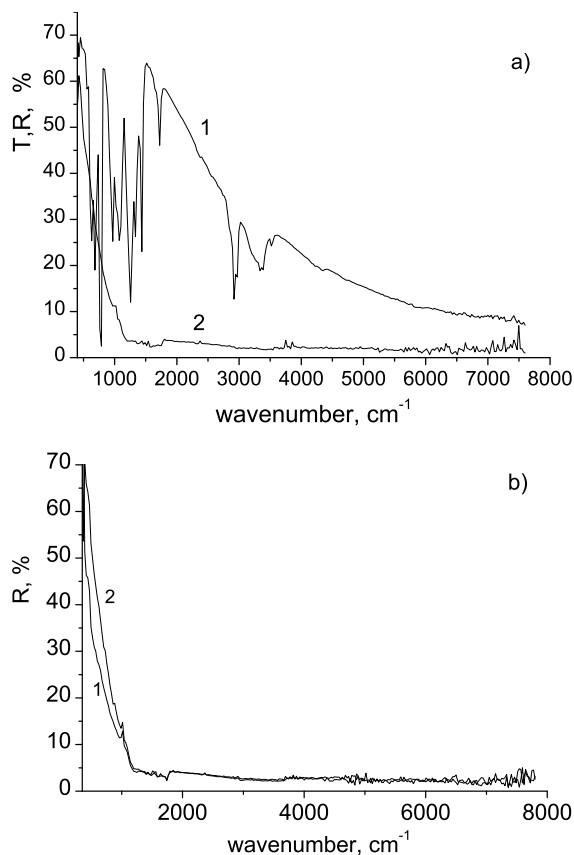


**Fig. 5.** IR spectra of CLON-Si and CYCAM-Si hybrids: *a*) curve 1 – transmission spectrum of a free film of CLON deposited from the  $\text{CCl}_4$  solution, curve 2 presents the reflection spectrum of the CLON-Si hybrid; *b*) reflection spectra of the CLON-Si (curve 1) and CYCAM-Si (curve 2) hybrids deposited from the water solution

separated from Si in the transmission regime (curve 1) and CLON-Si hybrid in the reflection regime (curve 2) in the  $400\text{--}8000\text{ cm}^{-1}$  wave number range. Figure 5, *b* shows the IR reflectance spectra for CLON( $\text{H}_2\text{O}$ )-Si (curve 1) and CYCAM-Si (curve 2) hybrids in the  $400\text{--}8000\text{ cm}^{-1}$  wave number range. Functional groups for all hybrids are documented in Table 2.

From the numerous and complex absorption bands observed in the FTIR transmission spectrum of a free layer and compared with literature data, it has been determined that, in the  $400\text{--}2000\text{ cm}^{-1}$  region, the absorption bands at about  $725\text{ cm}^{-1}$ ,  $1200\text{ cm}^{-1}$ , and  $1428\text{ cm}^{-1}$  are referred to  $\text{NH}_2$  bending modes and vibration at  $1650\text{ cm}^{-1}$  associated

to  $\text{NH}_2$  wag mode. Vibration bands at  $763\text{ cm}^{-1}$ ,  $820\text{ cm}^{-1}$ , and  $1300\text{ cm}^{-1}$  correspond to  $\text{CH}_2$ ,  $\text{CH}$ , and  $\text{CH}_2$  bending modes, respectively. The wide absorption band between  $1500\text{ cm}^{-1}$  and  $1700\text{ cm}^{-1}$  is due to the combination of  $\text{NH}$  bending and  $\text{CN}$  stretching groups. Presumably, the bands at  $650\text{ cm}^{-1}$  and  $1750\text{ cm}^{-1}$  correspond to  $\text{CCl}$  and  $\text{CH}_2\text{Cl}$  bending modes.

In the  $2300\text{--}4000\text{ cm}^{-1}$  range, the absorption bands at  $2900\text{--}3000\text{ cm}^{-1}$  are attributed to  $\text{CN}_n$  group vibrations. Between  $3300\text{ cm}^{-1}$  and  $3600\text{ cm}^{-1}$ , the absorption bands belong to  $\text{OH}$  and  $\text{NH}$  groups.

In the IR reflection spectrum (Fig. 5, curve 2) and Table 2, the modes with peaks at  $460\text{ cm}^{-1}$  and  $1080\text{ cm}^{-1}$  refer to Si-N stretching, and those at  $460\text{ cm}^{-1}$ ,  $1020\text{ cm}^{-1}$ ,  $3750\text{ cm}^{-1}$  are associated with Si-Si, Si-O-Si, Si-OH vibrations, respectively. The analysis of the peaks with modes at about  $1500\text{ cm}^{-1}$  and  $1700\text{ cm}^{-1}$  and between  $2100\text{ cm}^{-1}$  and  $2300\text{ cm}^{-1}$  show that they can be characterized by Si-Cl, Si-C and Si-H stretching modes. Thus, CLON molecules deposited on Si form Si-N, Si-Cl, Si-C, Si-H, and Si-OH bonds.

As for the comparison between the IR modes of functional groups immobilized on the Si surface from a CLON wafer, pentachlorophenol, and the mixed solution, it was found that there are some variations in the number, as well as in the distribution of functional groups, which allows one to control the PV properties of CLON-Si hybrids (Fig. 5, Table 2) Eff was 7–8% for CLON-Si hybrids deposited from mixed solutions at  $E = 20\text{--}60\text{ mV/cm}^2$  and about 6% at  $100\text{ mV/cm}^2$  (AM 1.5). At (AM 1.5), there are almost no difference in Effs of hybrids deposited from  $\text{H}_2\text{O}$  and  $\text{H}_2\text{O} + \text{C}_6\text{Cl}_5\text{OH}$  solutions.

The examination of the  $400\text{--}8000\text{ cm}^{-1}$  wave number range of IR reflection spectra of CYCAM-Si hybrid (Fig. 5, *b*) and the identification of the types of vibrational modes indicate the presence of characteristic bands associated with functional groups containing: (i) nitrogen – amines  $\text{NH}_x$  ( $x = 0, 1, 2$ ), amides  $\text{OCN}$ , cyanonitrile  $\text{CN}$ ; (ii) carbon and/or hydrogen-hydrocarbons  $\text{CH}_x$  ( $x = 1, 2, 3$ ); (iii) oxygen – hydroxyl  $\text{OH}$ , peptide  $\text{CO}$ ; (iv) phosphorus-phosphate  $\text{OPO}(\text{OH})_2$ .

In the last case, the most number of functional groups is not correlated with maximum Eff and its dependence on  $E$  (Fig. 3, curve 7, Table 2). However, such hybrid is interesting for two reasons: first, as



Table 2. Assignment of the infrared modes observed in ARD/Si hybrids

Mode	$\omega_{\text{FTIR}} \text{ (cm}^{-1}\text{)}$						
	CLON/Si					PRO/Si	B <sub>12</sub> /Si
	T	R				R	R
		CCl <sub>4</sub>	C <sub>6</sub> Cl <sub>5</sub> OH	H <sub>2</sub> O	H <sub>2</sub> O + C <sub>6</sub> Cl <sub>5</sub> OH		
Si-Si, N stretching	460	460	460	460	460	460	460
Si-Si			505	495	500	495	495
	520					520	520
	570		560			560	–
Si-H; Si-C; C-Cl	650	650				–	–
NH <sub>2</sub> bending; O-P-O, Si-C	725		725–740		750		710–725
CH <sub>2</sub> bending (rocking)	765					–	
CH bending	820		820			–	
Si-H <sub>2</sub>			850				
Si-CH <sub>3</sub>						–	880
Si-C	900		900				
Si-OH	1020	1020	1020	1060	1060	1020	1015
	1060		1060				
Si-N; Si-O-Si stretching	1080	1080	1080				1080
C-O-C	1130						
Si-H	1160					1150	1150
NH <sub>2</sub>	1200		1200				
CH <sub>2</sub> bending	1300					1300	1300
NH <sub>2</sub> bending	1400	1400	1400	1400	1400		
Si-Cl; C-N stretching; CH; NH bending, C-O	1500	1500	1500	1500	1500	1500	1540
Si-C; C=C; C-O stretching; NH <sub>2</sub> bending	1650	1650	1630		1630		1650
NH stretching	1700			1700		1725	1710
CH <sub>2</sub> Cl; COOH, CO, NCO	1750	1760	1750	1750	1760	1760	1750
Si-H							2000
Si-H stretching	2300	2300					2300
CH <sub>2</sub> stretching, CH	3000	2900			2900		2900
Si-CH <sub>3</sub>							3100
NH stretching	3500						
OH	3600		3600	3600	3600		
Si-OH		3750	3800		3800	3700	3750
C-H	4770		4700	4700	4700		4700
HN; HN <sub>2</sub>			6500	5700	5500–6500		6500

a variant for the solar energy conversation and, second, in biology and medicine fields as NDA and RNA analogues.

### 3.4. Final remark:

#### about operation principles of APD-Si hybrids

Although the understanding of the physical processes in all organic and organic-inorganic hybrid versions of solar cells remains limited, as compared to inorganic

solar cells, the last-decade investigations show the fundamental difference in the generation of photocarriers, recombination, and carrier transport. However, each novel structure requires the individual study. In the current case, the model assumes the presence of two materials: organic aromatic dye APD and inorganic Si patterned substrates with thicknesses about 20–30 nm and 300  $\mu\text{m}$ , respectively. The Si

zone structure is well known. It is a semiconductor with the indirect transition  $E_v - E_c - 1.12$  eV. For each organic material and hybrid structure including APD, the position of the HOMO–LUMO gap depends strongly on many factors such as Si bulk and its surface, solution composition, deposition regime, and organic molecular structure.

The results described in the previous subsections (3.1–3.3) show the hybrid formation of a chemisorbed layer on Si with barrier characteristics.

In this connection, the PL data and PL evolution spectra may be expounded in the following way:

(i) if the CLON–Si hybrid is deposited from H<sub>2</sub>O solution for the pyramid-like hybrid morphology, the HOMO–LUMO gap is not less 2.75 eV. It should be noted that this value is approximately similar for all APDs;

(ii) for the buried pyramids and net-like forms of hybrid morphologies, the HOMO–LUMO gap is not less 2.75 eV too. But there is at least one unoccupied molecular level at about 2.34 eV, i.e. LUMO-1. In addition, the 1.5 eV IR level is observed too;

(iii) for the branched and dendritic like morphologies, the PL peak has a redshift to 2.34 eV, i.e., the HOMO–LUMO gap is size-dependent.

In addition, if CLON–Si hybrids is deposited from the mixed, for example, H<sub>2</sub>O + C<sub>6</sub>H<sub>5</sub>OH + CH<sub>3</sub>OH solution (4, *b*), PL indicates the quenching as a result of the Cl<sub>2</sub> doping. It is well known that chlorine is a quencher for PL. In other words, the PL quenching may be the indirect possible way of sensitization and energy transfer from APD to Si, according to the Foster energy transfer mechanism [33]. The best quenching is shown by hybrids formed from the mixed solution without additional substances (Fig. 4, *b*, curve 3). Moreover, the Cl<sub>2</sub> doping increases the concentration of holes and ionized acceptors and shifts the Fermi level position toward the valence bandedge.

On the other hand, using the general diode principle of zone theory and assuming APD as an intrinsic semiconducting material ( $n^-$  or  $p^-$  types), the PV energy conversation is defined by the following processes: (i) creation as a result of the photon absorption into the Si surface (APD is a light window for Si); (ii) the carrier charge separation as a result of the potential gradient; (iii) the transport to the contacts.

After the photon absorption and the  $e - h$  pair creation, the electron from  $E_{cSi}$  may be lifted to the surface level at the interface (1.5 eV–2.0 eV) or onto one of the unoccupied molecular orbital of the acceptor fragment of a molecule, if there are the significant wave function overlap between the LUMO level and  $E_{cSi}$ . Then it is energetically favorable to reach the excited LUMO, and the transport to the upper contact is realized. In this case, the hole of  $E_{vSi}$  is transported to the base rear contact. The efficient carrier collection is determined by both the optimal upper self-organized net-like morphology and the diffusion length of the initial (start) Si material.

For CYCAM–Si hybrid, as was mentioned above, the photon absorption is the controlled antenna effect [34, 35]. However, the antenna-sensitized B<sub>12</sub> molecule is a very complex system with a long chain of the nucleotide component. This decreases the conductivity of the molecular layer.

Thus, it may be summarized that aromatic pharmaceutical drugs such as procainamide hydrochloride, cyanocobalamin (vitamin B<sub>12</sub>), and especially clonidine hydrochloride may be of interest for the use in PV and optoelectronics.

#### 4. Conclusion

The power energy conversation with efficiency from about 3.7% to 8.4% has been demonstrated in three different organic-inorganic hybrids under the incorporation of the functional groups of heteroatom aromatic drugs into the Si patterned surface during the room-temperature chemical bath deposition.

Exploiting the molecular self-organization and the molecular self-assembly for the morphological modification, sensitization, and functionalization of the Si surface and studying the effect of formation conditions and the molecular structure of APD on the PV performance and PL, the manipulation of the photovoltaic and optical properties of APD–Si hybrids has been realized.

In spite of the remaining limited understanding of physical processes and the operation of mechanisms, the classical model of generation of  $e - h$  pairs, charge separation, and transport is proposed. Such classical situation where the  $I_{sc}$  is a linear function of  $E$  (power energy irradiation), and  $V_{oc}$  has the logarithmic dependence on  $E$  with the further saturation, is realized in the CLON–Si hybrid formed from a H<sub>2</sub>O solution.

1. J.M. Buryak, Chem. Rev. **102**, 1271 (2002).
2. E.L. Aleksandrova, Semicond. **38**, 1115 (2004).
3. F. Tao, S.L. Bernasek, and Guo-Quin Xu, Chem. Rev. **109**, 3991 (2009).
4. M.A. Green, Physica E **14**, 65 (2002).
5. A. Goetzberger, C. Hebling, and H.W. Schook, Mater. Sci. Eng. R **40**, 1 (2003).
6. D.J. Milliron, I. Gur, and A.P. Alivisatos, MRS Bull. **30**, 41 (2005).
7. S. Gunes and N.S. Sariciftci, Inorg. Chem. Acta **361**, 581 (2008).
8. B.R. Saunders and M.L. Turner, Adv. in Colloid and Interf. Sci. **138**, 1 (2008).
9. S.P. Low, N.H. Voelcker, L.T. Canham, and K.A. Williams, Biomaterials **30**, 2873 (2009).
10. M. Wang, J.L. Coffey, K. Dorraj, P.S. Hartman, A. Loni, and L.T. Canham, Molec. Pharmac. **7(6)**, 2232 (2010).
11. Y. Liu, T.S. Niu, L. Zhang, and J.S. Yang, Natural Sci. **2**, 41 (2010).
12. Xiao Liu Chang. NanoBiomed. Eng. **3**, 73 (2011).
13. *Fundamentals of Silicon Integrated Device Technology. V.1. Oxidation, Diffusion, and Epitaxy*, edited by R.M. Burger and R.P. Donovan (Englewood Cliffs, N.J., Prentice Hall, 1967).
14. S.M. Sze, *Physics of Semiconductor Devices* (Wiley, New York, 1981).
15. K.E. Peterson, Proc. IEEE **70**, 420 (1982).
16. W. Lang, Mater. Sci. & Engin., R: Biomimetic Mater., Sens. and Syst. **R17**, 1 (1996).
17. S. Riad, Thin Solid Films **370**, 253 (2000).
18. M.M. El-Nahass, H.M. Zeyada, M.S. Aziz, and N.A. El-Ghamaz, Sol.-St. Electron. **49**, 1314 (2005).
19. C. Kelting, U. Weiler, T. Mayer, W. Jaegermann, S. Makarov, D. Wohrle, O. Abdallah, M. Kunst, and D. Schlettwein, Organic Electronics **7**, 363 (2006).
20. U. Weiler, T. Mayer, W. Jaegermann, C. Kelting, D. Schlettwein, S. Makarov, and D. Wohrle, J. Phys. Chem. B **108**, 19398 (2004).
21. I. Simkiene, J. Sabhataityte, G.J. Babonas, A. Reza, and J. Beinoras, Mater. Sci. Eng. C **26**, 1007 (2006).
22. B.K. Kang, N. Aratani, J.K. Lim, D. Kim, A. Osuka, and K.H. Yoo, Mater. Sci. Eng. C **26**, 1023 (2006).
23. Arroyo-Hernandez, Perez-Rigueiro, and Martinez-Duares. Mater. Sci. Eng. C **26**, 938 (2006).
24. M. Kittler, X. Xu, O.F. Vyvenko, M. Birkholz, W. Seifert *et al.*, Mater. Sci. and Eng. C **26**, 902 (2006).
25. J.M. Buryak, Phil. Trans. R. Soc. A **364**, 217 (2006).
26. S.P. Low, N.H. Voelcker, L.T. Canham, and K.A. Williams, Biomaterials **15**, 2873 (2009).
27. S.P. Low, K.A. Williams, L.T. Canham, and N.H. Voelcker, J. Biomed. Mater. Res. A **93**, 1124 (2010).
28. T.Ya. Gorbach, P.S. Smertenko, S.V. Svechnikov, and M. Kuzma, Thin Solid Films **511–512**, 494 (2006).
29. T. Gorbach, V. Kostylyov, and P. Smertenko, Mol. Cryst. Liq. Cryst. **535**, 174 (2011).
30. T.Ya. Gorbach, R.Yu. Holiney, L.A. Matveeva, P.S. Smertenko, S.V. Svechnikov, E.F. Venger, R. Ciach, and M. Faryna, Thin Solid Films **336**, 63 (1998).
31. M. Kuzma, G. Wish, E. Sheregii, T.Ya. Gorbach, P.S. Smertenko, S.V. Svechnikov, R. Ciach and A. Rakowska, Appl. Surf. Sci. **138–139**, 465 (1999).
32. M.D. Mashkovski, *Drugs* (Novaya Volna, Moscow, 2000) (in Russian).
33. R. Foster, *Organic Charge-Transfer Complexes* (Academic Press, London, 1969).
34. S. Huber and G. Calzaferri, Chem. Phys. Chem. **5**, 239 (2004).
35. O. Bossart, L. DeCola, S. Welter, and G. Calzaferri, Chem. Sur. J. **10**, 2391 (2004).

Received 20.05.13

Т.Я. Горбач, П.С. Смертенко, Є.Ф. Венгер

ДОСЛІДЖЕННЯ  
ФОТОВОЛЬТАІЧНИХ І ОПТИЧНИХ  
ВЛАСТИВОСТЕЙ САМООРГАНІЗОВАНИХ  
ОРГАНІЧНО-НЕОРГАНІЧНИХ ГІБРИДІВ  
НА ОСНОВІ АРОМАТИЧНИХ СПОЛУК  
ТА ПАТЕРНОГО КРЕМНІЮ

## Резюме

Ефект вбудовування функціональних груп ароматичних молекул на поверхню Si було досліджено за допомогою фотовольтаїчних та фотолюмінесцентних характеристик, інфрачервоної спектроскопії, скануючої електронної та оптичної мікроскопії. Для створення органічно-неорганічних гібридів тонкі шари (10–100 нм) гетероатомних ароматичних фармацевтичних препаратів, як: клонідина гідрохлориду, прокаїнаміда гідрохлориду та цианкобаламіну (вітамін B<sub>12</sub>), були сформовані осадженням хімічного розчину на патерну поверхню Si при кімнатній температурі та лабораторних умовах. Отримані гібриди показали, що: (i) перетворення сонячної енергії з ефективністю до 6–7% залежить від складу розчинника та морфології поверхні та інтерфейсу; (ii) найвища ефективність 8,4% спостерігалась у гібридів клонідина гідрохлорид – Si, отриманих у змішаних розчинах з товщиною у 30 нм та самоорганізованою ґратчастою морфологією поверхні; (iii) інтенсивна фотолюмінесценція у діапазоні 400–900 нм, профіль кривої люмінесценції та положення піка мають на увазі електронно-коливальне походження; (iv) наявність характерного діапазону пов'язується з функціональними групами, що містять нітроген (аміни NH<sub>x</sub> (x = 0, 1, 2)), амідні OCN, цианонітрили CN, карбон або карбогідроген (CH<sub>x</sub> (x = 1, 2, 3)), кисень (гідроксили OH, пептиди CO), галоген (хлоралкани) та фосфор (фосфати OPO(OH)<sub>2</sub>).